9. V. I. Tsypkin, V. N. Mineev, et al., "Investigation of the acceleration of copper plates by explosion products across a gap," Zh. Tekh. Fiz., 45, No. 3 (1975).
10. V. A. Ogorodnikov, S. Yu. Pinchuk, et al., "Experimental-theoretical investigation of the acceleration of plates by explosion products across a gap," Fiz. Goreniya Vzryva, 17, No. 1 (1981).

DETERMINATION OF THE SPALL STRENGTH FROM MEASURED VALUES OF THE SPECIMEN FREE-SURFACE VELOCITY

S. A. Novikov and A. V. Chernov UDC 539.412 :539.42

Measurements of the free-surface velocity on reflection of a nonstationary shock wave make it possible to obtain the data needed to determine the spall strength of a material σ_0, which is calculated from the expressions [1]

$$\sigma_0 = \rho_0 C_0 (W_0 - W_k)/2; \quad (1)$$

$$\sigma_0 = \rho_0 C_0 (W_0 - \bar{W}), \quad (2)$$

where ρ_0 is the initial density of the material; C_0, velocity of the plastic waves in it; W_0, maximum of the specimen free-surface velocity realized on arrival of the shock wave at that surface; W_k, value at the first minimum of the free-surface velocity time dependence; $\bar{W}$, mean velocity of the spall fragment. The values of W_0 and W_k are determined from the continuously recorded free-surface velocity measured by the capacitive transducer method [2]; W_0 can also be determined as the velocity of a thin artificial (prepared) spall fragment, i.e., a thin foil of the same material fitted tightly to the specimen; $\bar{W}$ is the usual mean spall velocity.

The literature does not contain any analysis of the limits of applicability of these expressions or the assumptions made in deriving them. We have therefore investigated the nature of the underlying assumptions and the limits of applicability of the equations derived.

Using the method of characteristics [3], let us consider the flow in a specimen subjected to spalling in the plane wave formulation. The X−T flow diagram is reproduced in Fig. 1a, where X is the Euler coordinate and T is time. We assume that the material fails instantaneously in a certain plane (the point F on the X−T diagram), as soon as the tensile stress in that plane reaches the value σ_0. This condition is first realized on the last C-characteristic OF of the centered rarefaction wave LOF formed when the shock wave SO reaches the free surface. The spall shock propagates from the fracture point F within the spall plate (to the right).

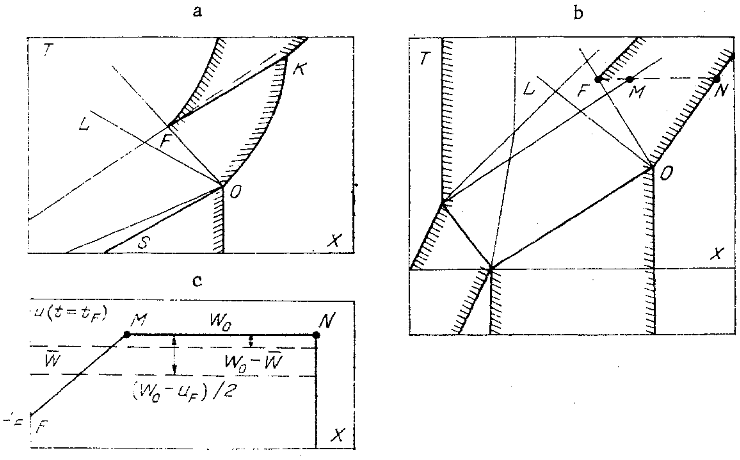

Fig. 1

Moscow. Translated from Zhurnal Prikladnoi Mekhaniki i Tekhnicheskoi Fiziki, No. 5, pp. 126-129, September-October, 1982. Original article submitted June 23, 1981.

0021-8944/82/2305-0703$07.50

It is assumed that the trajectory of this shock wave almost coincides with the C^+ characteristic FK passing through the fracture point; this assumption is legitimate if the amplitude of the shock wave is not too great and hence the spall strength σ_0 is low.

It is also assumed that the relation determining the behavior of the material takes the form of the usual equation of state $P=f(\rho, S)$, where ρ is density and S entropy. Consequently, the shear strength of the material is neglected. Then the equations of motion in characteristic form can be written as follows:

$$dX/dT = u + C,\ dP + \rho C du = 0; \tag{3}$$

$$dX/dT = u - C,\ dP - \rho C du = 0; \tag{4}$$

$$dX/dT = u,\ dS = 0, \tag{5}$$

where u is the mass velocity; $C^2 = (\partial P/\partial \rho)_S$ is the square of the speed of sound.

The final assumption is that the acoustic impedance ρC varies only very slightly along OF and FK and is approximately equal to $\rho_0 C_0$, where ρ_0 is the initial density of the material, and C_0 is the speed of sound at $P=0$.

Substituting $\rho_0 C_0$ for ρC in (3) and (4), we obtain the integrals along OF and FK:

$$P_F - P_0 - \rho_0 C_0 (u_F - u_0) = 0; \tag{6}$$

$$P_k - P_F + \rho_0 C_0 (u_k - u_F) = 0. \tag{7}$$

The boundary conditions take the form $P_F = -\sigma_0$, $P_0 = P_k = 0$, $u_0 = W_0$, $u_k = W_k$. From (6), (7), and the boundary conditions there follows equation (1).

The above conditions are not satisfied for all materials. For example, in the case of a material with well-expressed elastoplastic behavior possessing finite shear strength the acoustic impedance cannot be assumed to be constant, since the values of the elastic and plastic speeds of sound are sharply different. The flow pattern in the X–T plane may have a rather complex structure. The X–T plane is divided by the characteristics into a series of elastic and plastic regions. If information on the shear strength of the material is lacking, then it is impossible to make detailed calculations, and it can be stated only that the spall strength lies on the interval between the two values obtained from Eq. (1) when C_p (the plastic velocity of sound) and C_e (the velocity of longitudinal elastic waves in an infinite medium) are used as C_0. The difference in the value of σ_0, calculated for these two cases, is determined by the Poisson's ratio ν (at $\nu = 0.3$ it is $\approx 30\%$, $C_e/C_p \approx 1.27$).

For materials in which relaxation processes play a significant part the constitutive equation cannot be represented in the form $P=f(\rho, S)$, and the characteristic equations differ from (3)-(5), which can be demonstrated with reference to a simple example. Reference [4] is concerned with the propagation of plane waves in bars of an elastoplastic relaxing material. It is assumed that the plastic strain rate $\dot{\varepsilon}_p$, the stress σ and the total strain ε are related by the expression $E_0 \dot{\varepsilon}_p = g(\sigma, \varepsilon)$, where E_0 is Young's modulus. It is shown that for plane wave propagation the characteristic equations take the form

$$d\sigma - \rho_0 C_0 du = -g(\sigma, \varepsilon) dT,$$

$$d\sigma + \rho_0 C_0 du = -g(\sigma, \varepsilon) dT,\ d\sigma - E_0 d\varepsilon = -g(\sigma, \varepsilon) dT.$$

The importance of the relaxation processes is expressed in the fact that the right sides of the last relations make contributions to the integrals along OF and FK (Fig. 1a) comparable in magnitude to the contributions from the left sides. These terms give corrections to (1) that depend, generally speaking, on the boundary conditions. Consequently, it is not possible to obtain a single formula suitable for all flows.

Let us consider the question of the applicability of Eq. (2) for calculating the spall strength. We write Eq. (7) with allowance for the boundary conditions in the form $\sigma_0 = \rho_0 C_0 (W_k - u_F)$. This will coincide with Eq. (2) if we identify the mean spall velocity $\bar{W}$ with the mass velocity u_F in the spall plane immediately before fracture. Obviously, the relation $\bar{W} = u_F$ can be satisfied only under special loading conditions. For arbitrary loading greater or lesser deviations from this equality should be observed, and hence Eq. (2) may give an incorrect result. To illustrate this point, let us consider a colliding-plate flow in the case where the rarefaction wave has not yet overtaken the shock front as it reaches the free surface of the target. The X–T diagram for this flow is shown in Fig. 1b. In Fig. 1c we have plotted the distribution of mass velocities with respect to the spall coordinate, whence it follows that the mean spall velocity may considerably exceed u_F.

Apart from everything else, when Eq. (2) is used another source of error, associated with the experimental conditions, may play a part. In fact, measuring the mean spall velocity requires a large measuring base and hence a large spall fragment travel time, during which the disturbing influence of the target edges, located in the unloading zone, may make itself felt. This factor can lead to a lower value of the real spall velocity as compared with ideal experimental conditions. Since these edge effects are not usually monitored during the experiment, they can lead to unverifiable errors in calculating the spall strength from Eq. (2).

Thus, in cases where the shear strength or relaxation processes cannot be neglected, using Eq. (1) may lead to appreciable errors in determining the spall strength of the material. The use of Eq. (2) is justified only under special loading conditions, which are different for each specific type of equation of state.

LITERATURE CITED

1. S. A. Novikov, I. I. Divnov, and A. G. Ivanov, "Investigation of the fracture of steel, aluminum and copper under explosive loading," Fiz. Met. Metalloved., 21, No. 4 (1966).
2. A. G. Ivanov and S. A. Novikov, "Capacitive transducer method of recording the instantaneous velocity of a moving surface," Prib. Tekh. Eksp., No. 1 (1963).
3. R. Courant and K. O. Friedrichs, Supersonic Flow and Shock Waves, Wiley-Interscience, New York (1948).
4. L. E. Malvern, "The propagation of longitudinal waves of plastic deformation in a bar exhibiting a strain rate effect," Q. Appl. Math., 8, 405 (1951).

EXPERIMENTAL – THEORETICAL INVESTIGATION OF THE REBOUND OF SHORT RODS FROM A RIGID BARRIER

V. M. Boiko, A. I. Gulidov,
A. N. Popyrin, V. M. Fomin,
and Yu. A. Shitov

UDC 538.374

The present paper is a natural continuation of [1, 2], which gave a numerical simulation of the rebound of short homogeneous cylindrical and conical rods in the two-dimensional formulation. The integral criterion introduced in connection with the determination of the moment of rebound is applied not only to homogeneous rods but also to rods composed of different materials. The results of the numerical simulation are compared with the experimental data.

1. The physicomathematical formulation of impact problems, the definition of rebound, and the boundary and initial conditions were given in [1, 2] for homogeneous rods. We will now consider the case of a cylindrical rod composed of different materials impacting against a rigid barrier.

Problem 1. A cylindrical rod of length L_0 and radius R_0 consists of two materials. The materials are arranged in layers parallel to the axis of symmetry. The inner cylinder has the radius $R_0/2$. The thickness of the outer sheath is also $R_0/2$. The impact velocity $v_0 = 50$ m/sec. At the boundary between the layers the condition of perfect mechanical contact is satisfied. Mathematically, this condition reduces to the equality of the displacements and stresses at this boundary.

We will find the solution of the problem by the modified Wilkins method [2, 3]. In the numerical solution of the problem the calculation proceeds without explicit identification of the interface. The calculations were made for steel and copper layers with constants: $\rho_0 = 7.85$ g/cm^3, k = 170 GPa, $\mu = 80$ GPa, $y_0 = 1.2$ GPa – steel; $\rho_0 = 8.9$ g/cm^3, k = 139 GPa, $\mu = 46$ GPa, $y_0 = 0.3$ GPa – copper, where ρ_0 is the density of the material, k is the bulk modulus, μ is the shear modulus, and y_0 is the yield point.

Figure 1 shows the force acting at the rod–barrier interface as a function of time t for four combinations of materials (1 and 4 – solid steel and solid copper, respectively; 2 – inner cylinder copper, outer sheath steel; 3 – inner cylinder steel, outer sheath copper). We note that for the same initial impact velocity and the same geometry, the mass of the rods will be different and hence so will be the initial kinetic energy of the rods.

Novosibirsk. Translated from Zhurnal Prikladnoi Mekhaniki i Tekhnicheskoi Fiziki, No. 5, pp. 129-133, September-October, 1982. Original article submitted January 27, 1981.